FIRST STEREOSCOPIC CORONAL LOOP RECONSTRUCTIONS FROM *STEREO* SECCHI IMAGES

L. Feng,[1,2] B. Inhester,[1] S. K. Solanki,[1] T. Wiegelmann,[1] B. Podlipnik,[1] R. A. Howard,[3] and J.-P. Wuelser[4]

ABSTRACT

We present the first reconstruction of the three-dimensional shape of magnetic loops in an active region from two different vantage points based on simultaneously recorded images. The images were taken by the two EUVI telescopes of the SECCHI instrument on board the recently launched *STEREO* spacecraft when the heliocentric separation of the two space probes was 12°. We demonstrate that these data allow us to obtain a reliable three-dimensional reconstruction of sufficiently bright loops. The result is compared with field lines derived from a coronal magnetic field model extrapolated from a photospheric magnetogram recorded nearly simultaneously by *SOHO* MDI. We attribute discrepancies between reconstructed loops and extrapolated field lines to the inadequacy of the linear force-free field model used for the extrapolation.

Subject headings: methods: data analysis — Sun: corona — Sun: magnetic fields — techniques: image processing

Online material: color figures

1. INTRODUCTION

With the launch of NASA's *STEREO* mission in 2006 October, a new dimension of solar coronal observations has been opened. For the first time, objects above the solar surface can be perceived in three dimensions by analyzing the stereo image pairs observed with the SECCHI instruments on board the *STEREO* spacecraft and without making a priori assumptions about their shape. The two *STEREO* spacecraft orbit the Sun at approximately 1 AU near the ecliptic plane with a slowly increasing angle of about 45° yr^{-1} between *STEREO A* and *STEREO B*. Each spacecraft is equipped with, among other instruments, an EUV telescope (SECCHI/EUVI). For the objectives of the mission and more details about the EUVI telescopes see Wuelser et al. (2004) and Howard et al. (2007).

The major building blocks of the solar corona are loops of magnetic flux which are outlined by emissions at, e.g., EUV wavelengths. In principle, the magnetic field in the lower corona can be derived from surface magnetograms by way of extrapolations (e.g., Wiegelmann 2007). However, missing boundary values and measurement errors may introduce considerable uncertainties in the extrapolation results so that there is an obvious need for an alternative three-dimensional determination of the coronal magnetic field geometry. Among other goals of the mission, this requirement has been one of the drivers for *STEREO*.

Attempts for a three-dimensional reconstruction of the coronal magnetic field from EUV observations started long before *STEREO* data were available and date back more than a decade (Berton & Sakurai 1985; Kouchmy & Molodensky 1992). Here, we for the first time use two simultaneously observed EUVI images from the two *STEREO* probes and rigorously reconstruct loop shapes without any further assumptions about their temporal or spatial behavior from which earlier reconstructions employing consecutive images from a single spacecraft suffered

(Aschwanden et al. 2006). We compare the reconstruction results with field lines derived from linear force-free magnetic field models with variable α, the ratio of field-aligned current density to field strength (Seehafer 1978).

2. THE DATA

For our reconstruction we used EUV images at $\lambda = 17.1$ nm taken by the almost identical SECCHI/EUVI telescopes on board the two *STEREO* spacecraft at 2007 June 8 03:21 UT when the well-isolated NOAA active region 0960 was close to solar disk center. The line $\lambda = 17.1$ nm is emitted by the Fe IX ion which in thermal equilibrium forms at about 1.1 million K. At the time of these observations, the two *STEREO* spacecraft had a heliocentric separation of 11.807°. The precise spacecraft positions at the time of the observation are listed in Table 1.

For a comparison of our reconstruction with magnetic field lines we made use of a *SOHO* MDI magnetogram (Scherrer et al. 1995) taken only 9 s prior to the EUVI images. The active region is well isolated from neighboring field sources so that an extrapolation of the surface field is possible. MDI, however, provides only the line-of-sight field component, which for this bipolar region close to the disk center is almost identical to the radial field component on the solar surface. For this reason we can employ here only a linear force-free field model for the extrapolation of the magnetogram (Seehafer 1978).

3. THE RECONSTRUCTION

The first step in the stereoscopic reconstruction scheme is the isolation and identification of individual loops in each of the EUV images. In Figure 1 we show the portion of the EUV images containing the active region. The EUV structures were contrast enhanced by an unsharp mask filter. Next, individual loop structures were detected by a loop segmentation program. This program detects individual bright loops in an image by treating them as elongated intensity ridges (Inhester et al. 2007). For identification, the loop curves were enumerated. These assignments, e.g., a number i_A for a loop curve in image A, were made independently in each image.

To establish correspondences of projections $i_A \rightleftarrows i_B$ of the same loop across the images is the hardest part in the stere-

[1] Max-Planck-Institut für Sonnensystemforschung, Max-Planck-Strasse 2, 37191 Katlenburg-Lindau, Germany.

[2] Purple Mountain Observatory, Chinese Academy of Sciences, Nanjing, China.

[3] Naval Research Laboratory, Code 7660, 4555 Overlook Avenue, SW, Washington, DC 20375.

[4] Solar and Astrophysics Laboratory, Lockheed Martin ATC, 3251 Hanover Street, Palo Alto, CA 94304.

Parameter	A	B
Heliocentric distance (AU)	1.068788	0.958071
Sun's apparent radius (arcsec)	897.866	1001.625
Longitude (deg)	−4.277	7.524
Latitude (deg)	−0.293	0.095

Note.—Spacecraft longitude and latitude are given in the Heliocentric Earth Ecliptic (HEE) coordinate system.

oscopy procedure. For isolated loops they can sometimes be guessed by visual comparison of the image pair. Also, some guidance is provided by matching constraints which corresponding pairs of loop projections have to obey (Inhester 2006). Often, however, the visual comparison of loop structures does not yield unique correspondences. To disentangle the typically crowded active region loop ensembles we have developed a systematic scheme which determines correspondences with the help of magnetic field model calculations (Wiegelmann et al. 2005; Wiegelmann & Inhester 2006; Feng et al. 2007). The idea is to find three-dimensional field lines from a more or less accurate model of the active region magnetic field as a first approximation to the final loops whose projections are close to the loop projections identified in the images from spacecraft A and B. If a field line can be found with projections sufficiently close to a loop in both images, this is strong evidence that these loop curves represent projections of the same three-dimensional loop.

We quantify the proximity of a projected field line l to a loop curve i_A in image A, say, by the mean distance $C_A(i_A, l)$ between the two-dimensional curves in this image. The probability of a correspondence between a pair (i_A, i_B) of loop curves in image A and B can then be measured by $C = \frac{1}{2}\min_l[C_A(i_A, l) + C_B(i_B, l)]$. Here, the set of possible field lines l comprised all possible footpoint locations and a wide range of α-values from -0.01 to $+0.01$ Mm^{-1}. The field lines l here

only serve as a means to establish the correspondence; they are not intended to represent a consistent field model of the active region. The linear force-free field model used is only consistent if α is a global constant. Strictly speaking, the field lines l_{min} for which C attains the minimum are each from a different field line model as α turned out to differ for each loop pair.

In Figure 2 the inverse of C is shown for the loops in the northern half of the active region, $i_A = 0$ to 18 and $i_B = 0$ to 17. Some few loop combinations show a clearly enhanced $1/C$ and are thus much more probable than the majority of combinations (i_A, i_B). We accepted for a reconstruction only loop pairs with a value of C below 2 Mm. This corresponds to an average distance between the field line projection and the loop curves in each image of 2 pixels or less. When more than one combination was possible for one loop, the most probable one was taken such that each loop receives no more than one partner and the sum of C of all selected correspondences was minimized (Wiegelmann & Inhester 2006). In all, 20 pairs from Figure 1 could thus be identified.

The last step is the stereoscopic reconstruction of the three-dimensional loop from each accepted pair (i_A, i_B). This purely geometrical step often yields multiple solutions (Inhester 2006). These were discarded by retaining only the three-dimensional reconstruction closest to the best-fit field line l_{min}.

4. RESULTS

In Figures 3 and 4 we present two views of a set of reconstructed loops. Figure 3 shows the reconstructed loops (*yellow*) and the associated closest fit field lines (*red*) obtained by extrapolation from a position within a degree of the *STEREO A* spacecraft. As expected, loops and field lines agree relatively well from this perspective because they were chosen to be close in this projection. Figure 4 therefore provides a completely different view of the active region. This view shows that most of the loops cannot easily be approximated by planar curve
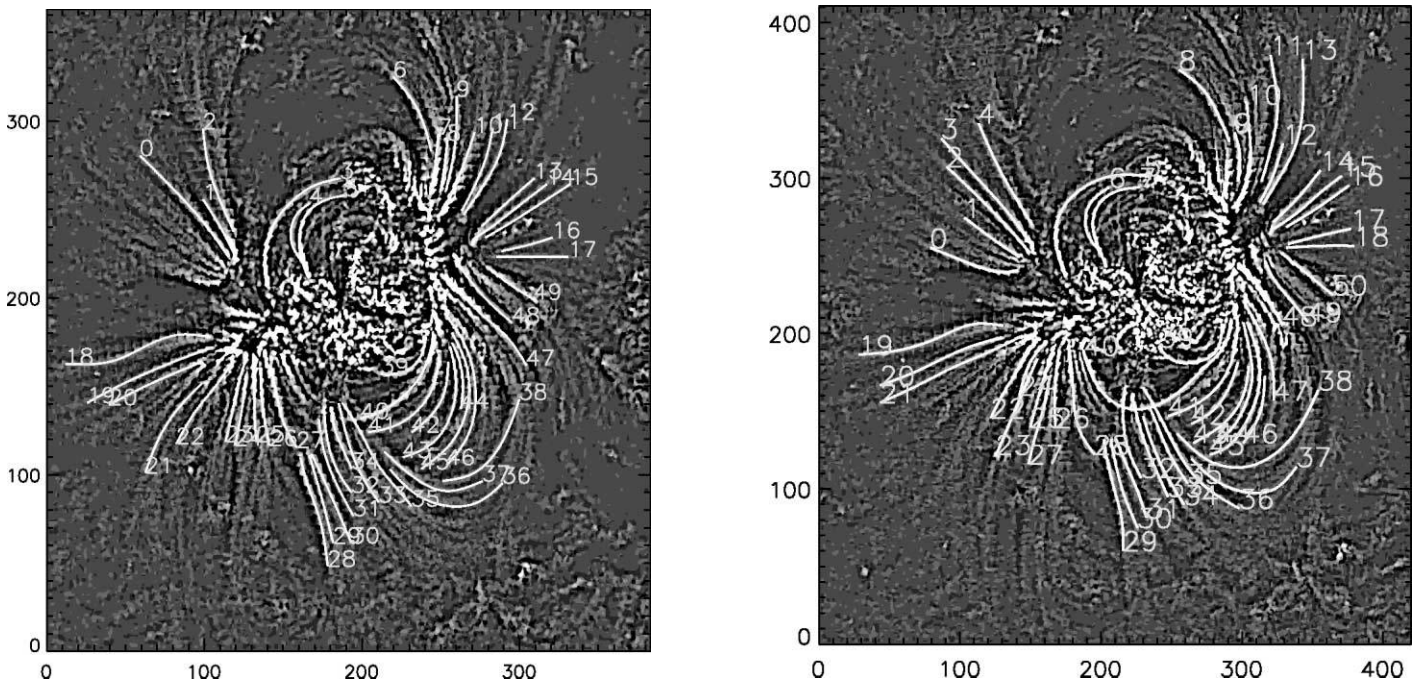

Fig. 1.—Contrast-enhanced zoom of EUVI images B (*left*) and A (*right*) of the NOAA AR 0960. Heliographic north is upward. The axes are scaled according to the image pixel size. Individual loop structures are emphasized by white curves and enumerated. Equal numbers do not imply a correspondence across the images. [*See the electronic edition of the Journal for a color version of this figure.*]
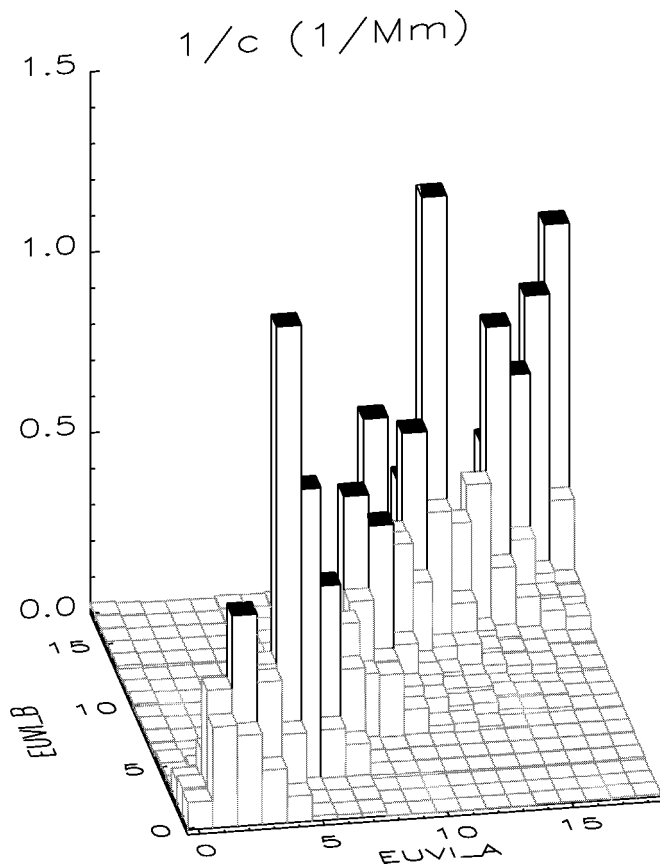
FIG. 2.—Proximity of loops identified in images A and B in Fig. 1. The proximity is expressed by the inverse of a distance measure C (see text). The loops from images A and B are arranged along axes "EUVI_A" and "EUVI_B" according to their respective identification number i_A and i_B. For each pair (i_A, i_B) the inverse of C is displayed by a column at the location of the loop pair in this matrix representation. Columns exceeding 0.5 Mm^{-1} have a black top. Here, only loops from the northern half of the active region were considered. [*See the electronic edition of the Journal for a color version of this figure.*]
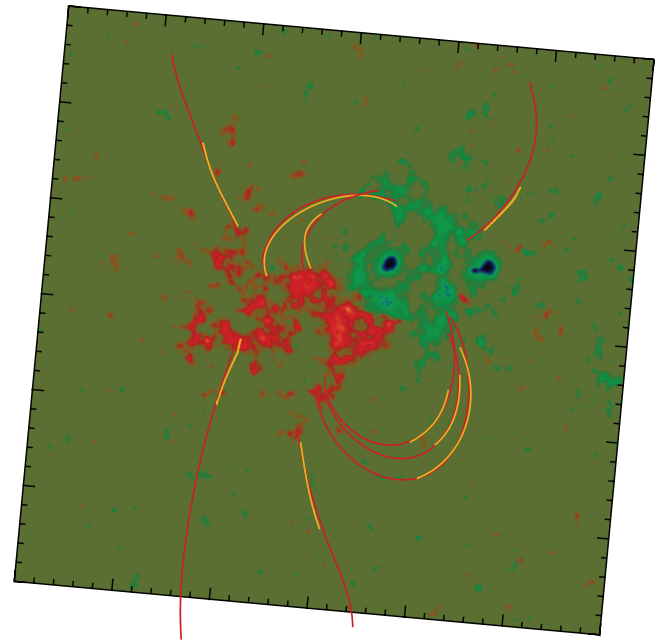

FIG. 3.—Vertical view of the three-dimensional reconstruction results from a viewpoint within a degree from the *STEREO A* spacecraft. Heliographic north is upward. The reconstructed loop sections are drawn in yellow, the closest fit field lines in red. The loop pairs (i_A, i_B) drawn are 4-2, 12-12, 5-3, 7-5 (northward part of this AR) and 45-45, 44-43, 42-42, 24-23, 30-29 (southward part).

segments. This geometrical simplification was often used for loop reconstructions in the past because a more involved shape could only rarely be resolved from previous observations. This figure also reveals deviations between the loops and field lines. For example, the loops on presumably open field lines appear to be more strongly curved than the corresponding field lines from the extrapolation.

We attribute this disagreement to a deficiency of the linear force-free field line extrapolation. For the closed field lines, the best-fit $|\alpha|$ values derived above fell in the range from 1.8 to 8.3×10^{-3} Mm^{-1} (see Table 2). For the open field lines, these values turned out to be smaller in magnitude, with values $|\alpha| < 2.5 \times 10^{-3}$ Mm^{-1}. As α is a global constant for the linear force-free field model, the influence of the stronger currents on the closed active region field lines is not accounted for on the open field lines. This may explain why the open field lines were calculated with less curvature than the corresponding stereoscopically reconstructed loops.

The loop reconstruction is also prone to errors, however. These may occur whenever a projected loop section in the images is directed tangentially to an epipolar line (Inhester 2006). For the viewing geometry of our observations, epipolar lines are nearly horizontal in the images and the critical part for closed, east-west orientated loops therefore lies more or less near their apex. Also, the open loop structures 16-19 in

image B and 17-20 in image A (see Fig. 1) suffer from this problem as they are orientated almost entirely horizontally in the images. We have therefore not attempted to reconstruct them even though a correspondence could well be identified.

In Figure 5 we display the reconstruction of loop (5, 3) (*yellow curve*), which shows by far the largest deviation from its best-fit linear force-free field line (*red curve*). For most other loops, this discrepancy is much less, although the agreement is rarely perfect. For some points along loop (5, 3), we also show error bars which represent the geometrical reconstruction error when the uncertainty for the loop projection in the images is assumed to be 1.5 pixels. In this case, the height of the loop top turns out to be ~1.5 times above that of the corresponding field line. This field line (the first entry in Table 2) again shows
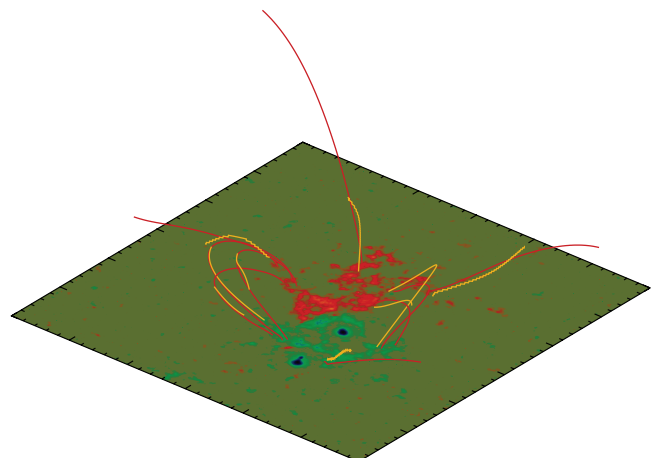

FIG. 4.—Same as Fig. 3, but seen from a viewpoint northeast of the active region. Heliographic north points to the lower left corner. The SECCHI instruments observed from approximately above.

Loop Pair (i_A, i_B)	$\|\alpha\|$ (10^{-3} Mm^{-1})	Height (Mm)	Length (Mm)
5, 3	1.8	71.9	229
7, 5	8.3	20.6	105
45, 45	2.3	58.2	253
44, 43	2.8	27.3	188
42, 42	2.8	57.2	210

a relatively small value $|\alpha|$. Since this α-value gave the best fit of linear force-free field lines to the loop projection in the images, we conclude that the linear force-free assumption is often not adequate (cf. Wiegelmann et al. 2005).

5. DISCUSSION AND OUTLOOK

We have demonstrated that EUV data from the new *STEREO* spacecraft allow us for the first time to make a reliable stereoscopic reconstruction of the spatial distribution of hot, magnetically confined coronal plasma and, by inference, provide a full three-dimensional view of the arrangement of coronal field lines. We find that linear force-free field models are helpful in establishing correspondences between the loops observed in the *STEREO* image pairs. The field lines from these linear force-free models need not be physical but only serve as a first-order approximation to the final loops. Realistic magnetic field models of the corona will have to be judged by their capability to yield field lines in agreement with the stereoscopically reconstructed loops. Our scheme to determine correspondences will become even more valuable when the stereo base angle grows and loop structures become more difficult to identify in the image pairs.

The reconstructions will also allow more precise analyses of emissions from loops. The observed brightness of EUV loops is, e.g., strongly modified by the inverse cosine of the angle between the line of sight and the loop's local tangent. This may, besides other effects, contribute to the enhanced EUV brightness of the lower loop segments commonly observed on the solar disk: these loop segments close to the loop's footpoints are more aligned with the radial direction and they make a small angle with the view direction. This may cause them to appear brighter than the loop top, which is viewed at more or less right angles.

Other applications have been proposed (Aschwanden 2005; Aschwanden et al. 2006). For example, the amount of twist of a reconstructed loop indicates how close the flux tube is to a kink instability. Török et al. (2004) found a threshold of about 3.5π in numerical simulations for the twist $\Phi = LB_\phi/rB_\parallel$. Here L is the length of the flux tube, $B_\parallel$ the toroidal field along its axis, and $B_\phi \simeq \alpha B_\parallel r/2$ the poloidal field at a radius r from the
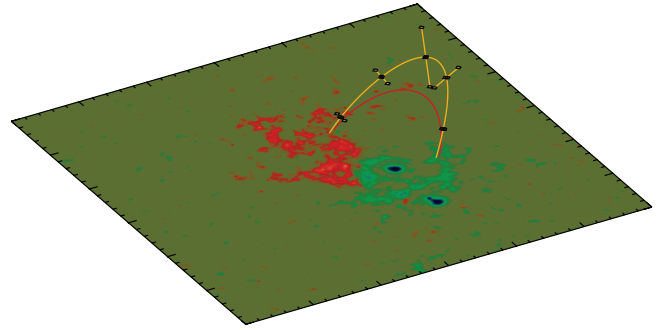

Fig. 5.—Example of a reconstructed loop with error estimates. The reconstruction is shown in yellow along with error bars. The associated best-fit linear force-free field line (*red curve*) is much lower in height.

flux tube center. In some cases it may be possible to resolve the number of turns n which a field line makes about the flux tube center from stereoscopic reconstruction and thus to determine the twist from $\Phi = 2\pi n$. Likewise, the twist is also related to α and L by $\Phi = \alpha L/2$. For the active region observed here, Table 2 gives values of $\Phi < 0.5$ well below the kink instability threshold.

Another perspective for stereoscopic loop reconstruction is the analysis of loop oscillations from a series of image pairs. The reconstructed loops will allow us to determine the transverse polarization of these oscillations (Aschwanden et al. 2002; Wang & Solanki 2004). Since the coronal magnetic field has a complicated geometry without symmetries, the frequency of these oscillations will significantly depend on this polarization. Note that these phenomena are invisible in the magnetic surface data and therefore cannot be retrieved from field extrapolations, which in addition require a stationary magnetic field.

REFERENCES

Aschwanden, M. J. 2005, Sol. Phys., 228, 339
Aschwanden, M. J., de Pontieu, B., Schrijver, C. J., & Title, A. M. 2002, Sol. Phys., 206, 99
Aschwanden, M. J., et al. 2006, Space Sci. Rev., DOI: 10.1007/s11214-006-9027-8
Berton, R., & Sakurai, T. 1985, Sol. Phys., 96, 93
Feng, L., et al. 2007, Sol. Phys., 241, 235
Howard, R., et al. 2007, Space Sci. Rev., in press
Inhester, B. 2006, preprint (astro-ph/0612649)
Inhester, B., Feng, L., & Wiegelmann, T. 2007, Sol. Phys., in press

Kouchmy, S., & Molodensky, M. M. 1992, Nature, 360, 717
Scherrer, P. H., et al. 1995, Sol. Phys., 162, 129
Seehafer, N. 1978, Sol. Phys., 58, 215
Török, T., Kliem, B., & Titov, V. S. 2004, A&A, 413, L27
Wang, T. J., & Solanki, S. K. 2004, A&A, 421, L33
Wiegelmann, T. 2007, J. Geophys. Res., in press, DOI: 10.1029/2007JA012432
Wiegelmann, T., & Inhester, B. 2006, Sol. Phys., 236, 25
Wiegelmann, T., Inhester, B., Lagg, A., & Solanki, S. K. 2005, Sol. Phys., 228, 67
Wuelser, J.-P., et al. 2004, Proc. SPIE, 5171, 111